PAPER • **OPEN ACCESS**

Enhancement of heavy ion track-etching in polyimide membranes with organic solvents

To cite this article: Kristina Froehlich *et al* 2022 *Nanotechnology* **33** 045301

View the article online for updates and enhancements.

You may also like

- Formulation of Sodium Hypochlorite Based Slurry for Copper-Cobalt Chemical Mechanical Planarization Process
Jenasree Hazarika and Prasanna Venkatesh Rajaraman
- The effect of sodium hypochlorite concentration on extraction of poly--hidroxy-butyrate (PHB) produced from soil bacteria *Burkholderia* sp B37
D Ratnaningrum, E S Endah, V Saraswaty et al.
- Efficacy of cold atmospheric pressure plasma jet against *Enterococcus faecalis* in apical canal of human single-rooted teeth: a preliminary study
K Saleewong, P Wanachantararak and P Louwakul

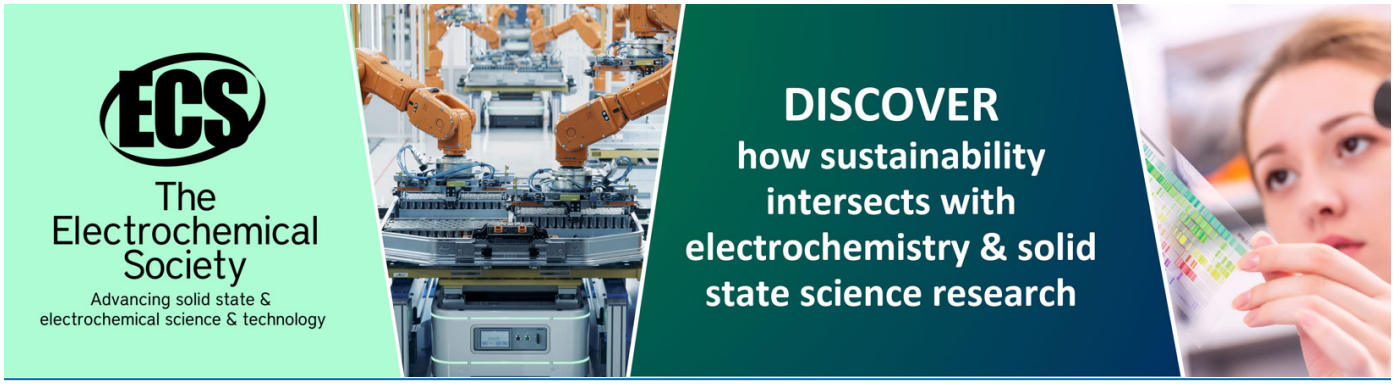

This content was downloaded from IP address 3.148.102.90 on 25/04/2024 at 05:45

OPEN ACCESS
IOP Publishing
Nanotechnology

Nanotechnology **33** (2022) 045301 (12pp)
https://doi.org/10.1088/1361-6528/ac2f5a

Enhancement of heavy ion track-etching in polyimide membranes with organic solvents

Kristina Froehlich[1], Martin Christoph Scheuerlein[1], Mubarak Ali[1,2], Saima Nasir[1,2] and Wolfgang Ensinger[1]

[1] Department of Material- and Geo-Sciences, Materials Analysis, Technische Universität Darmstadt, Alarich-Weiss-Str. 02, D-64287 Darmstadt, Germany
[2] Materials Research Department, GSI Helmholtzzentrum für Schwerionenforschung, D-64291, Darmstadt, Germany

E-mail: froehlich@ma.tu-darmstadt.de

Received 19 July 2021, revised 24 September 2021
Accepted for publication 13 October 2021
Published 2 November 2021

Abstract

The effect of organic solvents on the ion track-etching of polyimide (PI) membranes is studied to enhance the nanopore fabrication process and the control over pore diameter growth. To this end, two approaches are employed to investigate the influence of organic solvents on the nanopore fabrication in PI membranes. In the first approach, the heavy ion irradiated PI samples are pretreated with organic solvents and then chemically etched with sodium hypochlorite (NaOCl) solution, resulting up to ~4.4 times larger pore size compared to untreated ones. The second approach is based on a single-step track-etching process where the etchant (NaOCl) solution contains varying amounts of organic solvent (by vol%). The experimental data shows that a significant increase in both the bulk-etch and track-etch rates is observed by using the etchant mixture, which leads to ~47% decrease in the nanopore fabrication time. This enhancement of nanopore fabrication process in PI membranes would open up new opportunities for their implementation in various potential applications.

Supplementary material for this article is available online

Keywords: heavy ion irradiation, track-etching, organic solvents, nanopores, polyimide

(Some figures may appear in colour only in the online journal)

1. Introduction

Recently, synthetic nanopores are gaining much attention because of their implementation for the miniaturization of biosensing devices in the field of bio/nanotechnology [1–3]. Moreover, the nanoporous membranes are frequently employed for molecular separation and purification processes as well as energy conversion systems [4–10]. Depending on the desired application, the nanopore dimensions such as size, shape, surface properties as well as the utilized membrane materials can be tuned to fulfill specific requirements. Solid-state materials employed for the nanopore fabrication can be subdivided into nitrides (silicon or boron nitride), oxides (silicon dioxide and aluminum oxide), polymers such as polyethylene terephthalate (PET), polycarbonate (PC) and polyimide (PI), 2D materials (graphene), glass (borosilicate, quartz) and nanotubes (carbon nanotubes) [11–19]. Various methods were implemented to generate synthetic nanopores, for example focused ion beam (FIB) and focused electron beam (FEB) sculpting, dielectric breakdown, laser assisted pulling of capillaries, plasma etching or track-etching technique [20–27]. Recently, Chen and Liu have compared and summarized the limitations of various solid-state nanopore fabrication techniques [28]. For example, the FIB and FEB techniques can only be employed to fabricate nanopores in very thin (<100 nm) membranes. Moreover, FIB and FEB, laser assisted pulling of capillaries and plasma etching are not

Original content from this work may be used under the terms of the Creative Commons Attribution 4.0 licence. Any further distribution of this work must maintain attribution to the author(s) and the title of the work, journal citation and DOI.

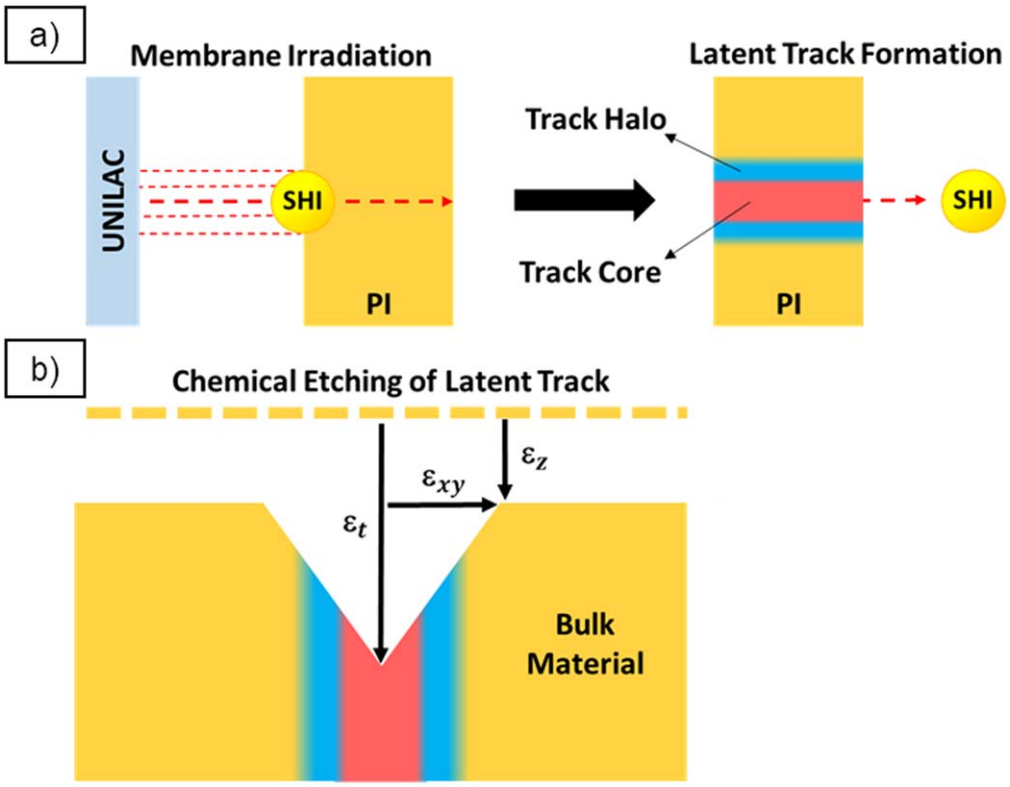

Figure 1. Illustration of (a) the irradiation of a polymer membrane with swift heavy ions to generate latent tracks. (b) The chemical etching of latent tracks to fabricate nanopores due to different etch rates of the bulk material ε_{xy} and the etch rate along the track ε_t.

cost-effective because they rely on several manufacturing steps as well as expensive instrumentation, preventing a mass production of nanopore-based devices [22, 26–29]. In contrast, dielectric breakdown is a simple and cheap method. But the generated nanoporous membranes show different effective thicknesses, which affects the sensing properties [22, 29]. On the other hand, track-etching technique enables the fabrication of low-cost, homogeneous and high-efficient nanopores on a massive scale. Furthermore, the track-etched nanopore exhibit mechanical/chemical stability to modify the pore surface characteristics [28, 29].

In the first step, the polymer membranes are bombarded with swift heavy ions (SHI) to produce highly localized and irreversible damages. The trajectories of the heavy ions through the polymer are called latent tracks (figure 1). These damage zones are a few nanometers in diameter along their trajectories (halo). The mechanism of track formation in polymers is complex because in addition to the primary processes, the secondary processes such as the formation of radicals and chemical reactions are also involved during heavy ion irradiation, which affects the chemical nature of the damages along the trajectories and the etchability of latent tracks. Latent tracks are more vulnerable for chemical etching than the rest of the material. They can be transformed into nanopores by selectively removing the damaged zone through track-etching technique by using a suitable chemical etchant depending on the nature of the polymer membrane (figure 1). For example, the latent ion tacks in PET and PC membrane can be easily removed with sodium hydroxide (NaOH) [30, 31]. The pore diameter can be tuned by varying the etchant concentration, temperature and the duration of the etching process. Moreover, several parameters have been adjusted such as exposure to UV light, variation of potential across the membrane and also addition of surfactants and different solvents in the etching solution to enhance the homogeneity and etching rate [7, 32–36].

Among the various commercially available polymers, PI is very attractive in a wide field of applications because of its excellent physical, chemical, electrical and mechanical properties at low and high temperature extremes [37–41]. Due to the high resistance and stability even under harsh conditions, nanoporous PI membranes are highly suitable for sensing applications ensuring a long life-time of the sensor and low costs of the raw material. Also, ion currents through nanopores in PI membranes exhibit a stabile current signal in contrast to nanopores in PET membranes, which show ion current fluctuations due to dangling ends at the pore openings [25]. However, the fabrication of nanopores in PI membranes is difficult and requires harsh etching conditions. Usually, a chemical etchant based on sodium hypochlorite (NaOCl) solution containing 12%–13% active chlorine content with pH $>$ 12 is used for ion track-etching of PI membranes at high temperatures (50 °C) [42–44]. Previously, several studies have been published on the track-etching of PI using NaOCl as an etching solution. It has been shown that the pH and the concentration of active chlorine of the NaOCl solution play a crucial role in the track-etching process [44, 45]. For example, Trautmann and coworkers have

investigated the influence of the etching solution pH value on the pore geometry. They have observed that the bulk-etch rate increases exponentially with the pH, while the track-etch rate has only a weak linear dependence on pH of the etchant [44]. Klintberg *et al* described the effect of decomposition of aqueous NaOCl solution during the etching process on the etch rates and nanopore shape. Note that the aqueous NaOCl is unstable and gradually deteriorates on exposure to heat, light and variation of solution pH [45].

To keep the bulk-etch rate and the latent track-etch rate constant during the ion track-etching of PI membranes, it is important to reduce the NaOCl solution decomposition caused by heat and pH changes during the etching process. This can be achieved by increasing the etch rates and decreasing the etching time. Previously, a combination of an etchant and a strong oxidizer such as potassium permanganate or hydrogen peroxide has been used to enhance the track-etch rate [30, 46]. To the best of our knowledge, so far the effect of organic solvents on the chemical track-etching of PI membranes has not been investigated.

In this study, we explore the effect of organic solvents on the track-etching of PI membranes. A variety of solvents such as acetonitrile (ACN), dichloromethane (DCM), *N,N*-dimethyl formamide (DMF), dimethyl sulfoxide (DMSO), ethanol (EtOH), methanol (MeOH), 2-propanol (i-PrOH), tetrahydrofuran (THF) and ethyl acetate (EAc) are investigated in combination with chemical etchant (NaOCl, 12% Cl). Two approaches are examined to fabricate nanopores in PI membranes. In the first approach, PI samples are first soaked in the organic solvent, followed by chemical etching of the ion tracks with NaOCl solution. In the second approach, track-etching is performed with etchant mixtures having different ratios (by vol%) of NaOCl and organic solvents. Moreover, the track-etching is also studied at different temperatures ranging from 23 °C to 50 °C. The influence of organic solvents on the nanopore diameter is analyzed through scanning electron microscopy (SEM).

2. Materials and methods

2.1. Materials

Acetonitrile (ACN, ⩾99.5%, VWR chemicals), dichloromethane (DCM, ⩾99.5%, Promochem), *N,N*-dimethyl formamide (DMF, ⩾99.8%, Merck KGaA), dimethyl sulfoxide (DMSO, ⩾99%, Alfa Aesar), ethanol (EtOH, ⩾99.5%, PanReac AppliChem), methanol (MeOH, 99.5%, PanReac AppliChem), 2-propanol (*i*-PrOH, > 99.9%, Selectipur, BASF), tetrahydrofuran (THF, ⩾99.9%, Merck KGaA), ethyl acetate (EAc, ⩾99.9%, Roth), sodium hypochlorite solution (NaOCl, 12% Cl, Roth), potassium chloride (KCl, ⩾99%, PanReac AppliChem) and potassium iodide (KI, ⩾99%, Roth) were used as received. All aqueous solutions were prepared using Milli-Q water (Millipore, resistance of >18.2 MΩ cm).

2.2. Fabrication of ion track-etched nanopore membranes

Polyimide foils (PI, Kapton 50 HN, DuPont) with a thickness of 12 μm were irradiated with SHIs (Au^{25+}, energy: 11.4 MeV u^{-1}) at the universal linear accelerator (UNILAC) at GSI Helmholtz Center for Heavy Ion Research, Darmstadt (Germany) [47].

To investigate the etch rate of the bulk material, nanopores were fabricated in PI membranes using symmetric track-etching technique [44, 45, 48]. The irradiated PI membrane (10^7 ions cm^{-2}) was placed between two chambers of home-made conductivity cells. The etching solution is filled in both cells to perform the symmetric etching of the ion tracked membrane. For this purpose, two approaches were investigated: in the first approach, a two-step etching process was performed. In this case, a pretreatment of the PI membrane was performed by soaking it in an organic solvent (ACN, THF, DMF, DMSO, EtOH, MeOH) for ∼1 h at 50 °C in a closed glass beaker. Then the pretreated membrane was symmetrically etched with the etchant solution (NaOCl with 12% active chlorine, pH 12.3 ± 0.1) for 45 min at 50 °C in the conductivity cells. In the second approach, the track-etching of irradiated PI membranes was performed without any pretreatment with organic solvents. However, the etching solution was prepared by mixing different ratios of the NaOCl and organic solvent (by vol%). The untreated membrane was fixed in between the two compartments of the conductivity cell and the etchant (NaOCl/organic solvent by vol%) was added in both compartments. Two gold electrodes were placed on both sides of the PI membrane and a constant potential of −1 V was applied with a Keithley 6487 picoamperemeter/voltage source (Keithley Instruments, Cleveland, OH, USA) across the membrane to monitor the current flow during the etching process. The current remains zero while the ion tracks are not completely etched through. After breakthrough, the current increases continuously. The etching was performed at different temperatures (23 °C, 35 °C and 50 °C) with different volumes of the organic solvent (5%, 10%, 20%, 30% and 40%) for various etching times ranging from 20 to 45 min. In both approaches, the conductivity cells were covered during etching to reduce the evaporation and decomposition of NaOCl caused by light, as well as the evaporation of any solvents. After etching, the membranes were washed with a stopping solution (1 M KI) to neutralize the etchant and several times with purified water to remove the residual salts.

Symmetric and asymmetric track-etching technique was used to fabricate single nanopore membranes for current–voltage (*I–V*) measurements and PI membranes with an ion track density of 10^7 ions cm^{-2} for nanopore profile analysis under SEM [43, 48]. The etching was performed until breakthrough (single nanopore membranes) and for 45 min (multi nanopore membranes) at 50 °C with the PI foil fixed between two chambers of the conductivity cells. In contrast to symmetric etching procedure, for asymmetric etching only one side of the cell contained the etchant, while the other side of the cell was filled with 1 M KI stopping solution. If the etchant was a mixture of NaOCl/solvent (9:1), then the

stopping solution also contained the same volume of the organic solvent as the etchant.

2.3. SEM analysis

SEM measurements were performed using a *Philips* XL30 FEG at an acceleration voltage of 25 kV. The etched membranes were fixed on the sample holder with sticky carbon pads. To ensure electric conductivity, a thin Au layer was evaporated on the samples using a *Quorum* Q300TD sputter coater. The sputter current was set to 30 mA for 60 s.

2.4. Profilometry

Profilometry was conducted on a *Bruker* Dektak XT using a stylus with a tip radius of 12 μm, applying a force of 5 mg. The membranes were fixed on glass slides with a small drop of deionized water. For each sample, three line scans were performed, comparing the height of the pristine polymer with that of the etched regions to determine the etch rate ε_z of the bulk material.

2.5. Contact angle measurements

Contact angle measurements were performed with a drop shape analyser OCA produced by Krüss GmbH. 3 μl droplets of (a) 12% NaOCl solution were placed on PI membranes which were soaked for 90 min at room temperature in a closed beaker filled with H_2O, ACN, THF, EtOH or DCM, and (b) H_2O, NaOCl solution and NaOCl/solvent (9:1) mixed solutions were placed on untreated PI membrane. The contact angle was determined using the software SCA20, by averaging the sessile drop shape of at least 3 droplets per measurement.

2.6. Current–voltage (*I–V*) curves of single nanopore membranes

The PI single nanopore membrane was fixed between two chambers of the conductivity cell. The chambers were filled with 0.1 M KCl solution. A grounded (stainless steel) Faraday cage shielded the cell from electrical interference. The *I–V* curves were measured using a Keithley 6487 picoamperemeter/voltage source (Keithley Instruments, Cleveland, OH, USA). A scanning triangular voltage, from +2 to −2 V in 100 mV steps was applied between two Ag/AgCl electrodes (wire with 1 mm diameter). Every data point was the average value of at least six individual measurements.

3. Results and discussion

It was previously shown that organic solvents have the potential to generate sub-nanometer nanopores in PI membranes by selective dissolving of the ion track without damaging the bulk material [5, 6]. In this study, the role of organic solvents either via membrane pretreatment with organic solvent or by adding it in the chemical etching (NaOCl) solution is thoroughly investigated to improve the fabrication process of nanopores in ion tracked PI membranes in terms of faster pore formation and better control of the pore diameter growth.

3.1. Symmetrical etching of pretreated PI membranes

Heavy ion irradiated PI membranes (10^7 ions cm^{-2}) are pretreated with organic solvents including ACN, THF, DMSO, DMF EtOH and MeOH followed by symmetrical chemical etching with commercially available NaOCl at 50 °C. Our previous reports show that the nanopores formed in the pretreated membrane are in the sub-nanometer range. As these dimensions are challenging to resolve by means of SEM, especially due to the necessity of coating the sample with a conductive layer, no nanopores are observed in the SEM images (figure S1 available online at stacks.iop.org/NANO/33/045301/mmedia). Following the pretreatment step, nanopores in the solvent treated membranes are fabricated by symmetric chemical track-etching with NaOCl for 45 min at 50 °C (figure 2). The SEM images of the chemically etched nanopores are shown in figure 3. From the SEM analysis, we have observed that almost all chemically track-etched PI samples pretreated with organic solvents (except MeOH) resulted in a significant increase of the pore diameter as shown in table 1. The SEM data showed only a 16% increase in the pore diameter in the case of MeOH-pretreated sample compared to the untreated one. Whereas, the pore diameters were almost doubled in size for PI samples pretreated with ACN (+105%) and EtOH (+107%). The highest effect of pretreatment is observed in the case of THF (+240%), DMF (+284%) and DMSO (+347%) generating pores in the micrometer range after only 45 min of etching.

Although the pretreatment step results in most of the cases an impressive pore diameter increase compared to a non-treated PI sample, the pore opening shape is very conspicuous. The borders of the pore walls of the samples pretreated for example with THF (figure 3(e)) and DMSO (figure 3(g)) appear unsmooth, rough and irregular, or even have a crack in the EtOH-treated sample (figure 3(d)). Moreover, for almost all solvent-treated samples (except MeOH), the nanopores are elliptical shaped. Apel *et al* reported that elliptical shaped nanopores in polymer membranes can be caused by the anisotropy in biaxially stretched polymer materials, where preferential orientation of macromolecular chains and anisotropic residual mechanical stress can contribute to different etch rates along and across the directions of stretching [49]. The chemical etching in an etchant filled in a closed beaker leads to the fabrication of nanopores with circular shaped pore openings compared to the samples fixed between the chambers of the conductivity cell (figure S2). This suggests that the steric properties and mechanical forces have to be considered during pore fabrication. However, elliptical shaped nanopores could be interesting for example in ultrafiltration processes, where such pore shape increases the permeability of the membrane while keeping the selectivity [50].

Since polymers tend to swell in liquids, there are at least two possibilities how organic solvents might affect the

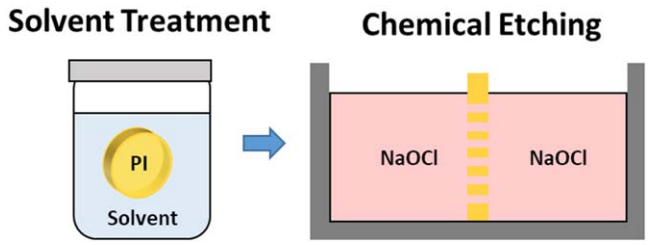

Figure 2. Experimental set-up for the fabrication of nanopores in PI membranes by using a two-step etching method at 50 °C.

chemical track-etching process [51, 52]. Firstly, organic solvents might be indirectly involved in the ion track dissolving/softening by only swelling the polymer membrane, making the polymer chains wider and more vulnerable for imide rings cleavage by the active chlorine. Due to swelling, the accessibility of the electrophilic centers is increased (shielding in tight and dense polymer structures is higher than in swollen ones), which results in a faster etching process. Secondly, the organic solvents might also be directly involved in the dissolving and softening of the ion track core. Since the etching step is performed immediately after solvent treatment, we assume that organic solvent residues are still adsorbed/embedded in the polymer bulk material. It is possible that these molecules would enhance and accelerate the etching process, e.g. by creating a more aggressive etchant (without affecting the pH value significantly). Figure S3(a) shows that the NaOCl solution leads to changes in the contact angle after soaking PI membranes for ~90 min at room temperature in different solvents compared to an untreated sample. However, there is no clear correlation between the resulting pore diameter and contact angle, which suggests that the wettability of the membrane surface is not the main reason of the increased etch rates.

3.2. Symmetrical etching with NaOCl/organic solvent mixtures

3.2.1. Influence of organic solvent on bulk-etch and track-etch rates. Further experiments were performed to investigate the effect of organic solvents during chemical etching on the etch rates. To this end, the etchant is prepared by mixing NaOCl and organic solvent in a ratio of 9:1, meaning that the etching solution contains 90 vol% of NaOCl and 10 vol% of an organic solvent. The PI membranes are symmetrically etched for 45 min at 50 °C with the etchant mixture (figure 4).

Figures 5(a)–(d) show the SEM images of PI membranes etched with NaOCl, NaOCl/ACN, NaOCl/THF and NaOCl/EtOH, respectively. The chemical etching of the PI membrane using commercially available NaOCl generates pores with a diameter of 0.43 ± 0.02 μm after 45 min. The addition of organic solvents in NaOCl solution leads to an increase of the pore diameter, although all other experimental conditions stay the same. In the presence of ACN, THF and EtOH, the diameters of track-etched nanopores are 1.22 ± 0.04 μm, 1.70 ± 0.06 μm and 2.32 ± 0.13 μm, respectively. It is evident that the addition of ACN, THF and EtOH to the etchant leads to a ~3-times, ~4-times and ~5.4-times increase in the pore diameter compared to PI samples etched with pure NaOCl solution, respectively. Comparing these results with figure 3 and table 1, the mixture of NaOCl solution and organic solvents generates larger pore diameters than the etching after pretreatment with ACN, THF and EtOH. Moreover, the pores obtained with the NaOCl/organic solvent mixture are of circular shape, with a more uniform diameter distribution, while exhibiting remarkably smooth pore openings.

To determine the etch rates $\varepsilon_{xy}^{\text{etchant}}$ for the etchant mixtures, we analyzed the pore diameter in dependence of the etching time (figures 5(e), S4–S7). The pore diameter depends on the etch rate of the bulk material $\varepsilon_{xy}^{\text{etchant}}$ at the latent track position. Under the same experimental conditions, the etch rates are $\varepsilon_{xy}^{\text{NaOCl}} \approx 16 \pm 1$ nm min^{-1}, $\varepsilon_{xy}^{\text{NaOCl/ACN}} \approx 28 \pm 3$ nm min^{-1}, $\varepsilon_{xy}^{\text{NaOCl/THF}} \approx 54 \pm 7$ nm min^{-1} and $\varepsilon_{xy}^{\text{NaOCl/EtOH}} \approx 65 \pm 9$ nm min^{-1}. The etch rates ε_{xy} determined from SEM images are in good agreement with the results of ε_z obtained by profilometry (figure S9). It is worth mentioning that the intersection of the linear fit for NaOCl/ACN, NaOCl/THF and NaOCl/EtOH mixtures with the *y*-axis is not at zero. One reason is that the etching is not a linear process. It takes some time before a pore opening is formed and the diameter starts to rise. Furthermore, we started the chemical etching with an etchant temperature of 23 °C (room temperature), which means that the etching solution has to warm up until 50 °C while the etching is already in progress.

To determine the etch rate along the latent track ε_t, a potential is applied across the membrane during chemical etching to monitor the track-etching process. The current value stays around zero until the breakthrough occurs. As soon as the etching solutions from both polymer sides meet in the center of the membrane, the nascent nanopore is generated and an ion flow through the membrane is possible. A current increase is detected (figure 5(f)). Note that the current value depends on the number of latent tracks in the etched membrane area and the number of breakthroughs. Since the latent track distribution after SHI irradiation of the PI foil is statistical and the polymer has crystalline and amorphous structures, the etch rate ε_t can vary between the tracks. For this reason, the current values in figure 5(f) show the summarized currents versus time. When using NaOCl as etching solution, latent tracks with the highest etch rate ε_t show a breakthrough after ~32 min. Adding small amounts of EtOH to the etching solution can decrease the breakthrough time to ~30 min. Addition of ACN and THF to the NaOCl solution further reduces the breakthrough time to ~17 min and ~22 min, respectively. The etch rate $\varepsilon_t^{\text{etchant}}$ can be estimated with equation (1) [7, 44]

$$\varepsilon_t^{etchant} = \frac{l}{2t}. \quad (1)$$

With a membrane thickness l of 12 μm and the time required to reach breakthrough t, the etch rates along the latent tracks are $\varepsilon_t^{\text{NaOCl}} \approx 188$ nm min^{-1}, $\varepsilon_t^{\text{NaOCl/EtOH}} \approx 200$ nm min^{-1}, $\varepsilon_t^{\text{NaOCl/ACN}} \approx 353$ nm min^{-1} and $\varepsilon_t^{\text{NaOCl/THF}} \approx 273$ nm min^{-1}. These results show that the addition of organic solvents to the NaOCl etching solution does not only increase the etch rate of the bulk material ε_{xy}, but also the etch rate along the latent tracks ε_t, reducing the fabrication time of

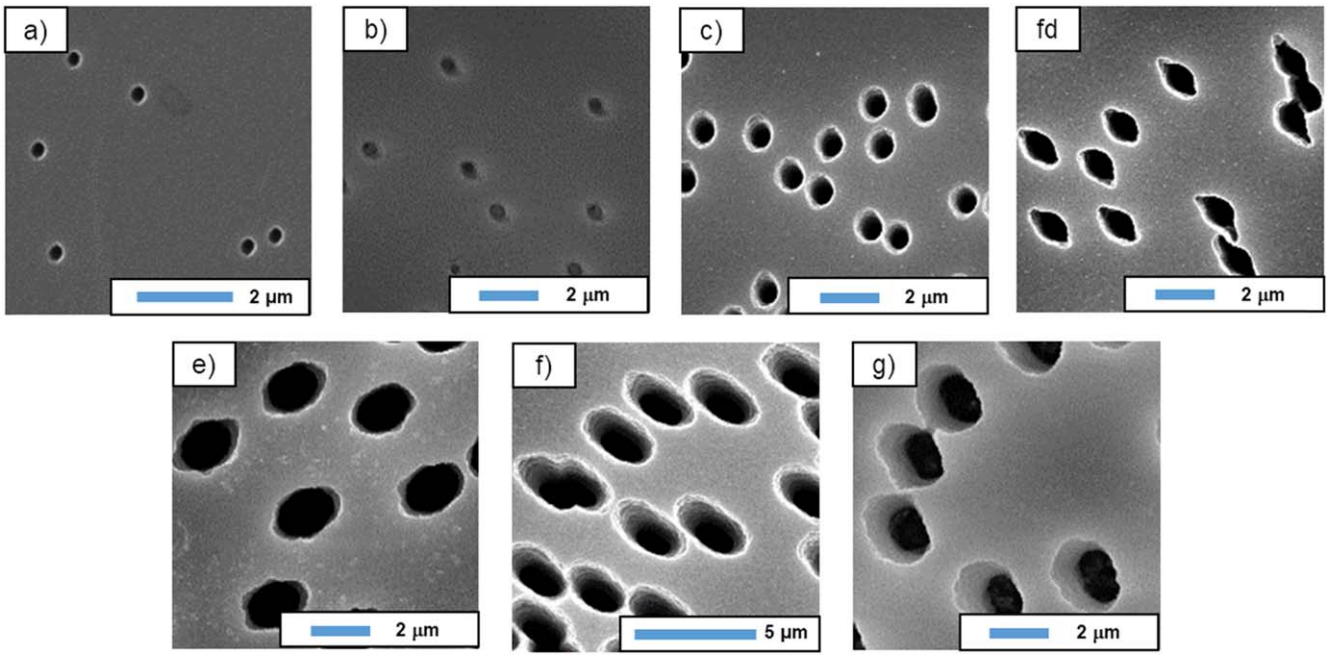

Figure 3. SEM images of PI membranes (10^7 pores cm^{-2}) etched symmetrically using a two-step etching process (a) no solvent treatment, (b) MeOH, (c) ACN, (d) EtOH, (e) THF, (f) DMF and (g) DMSO.

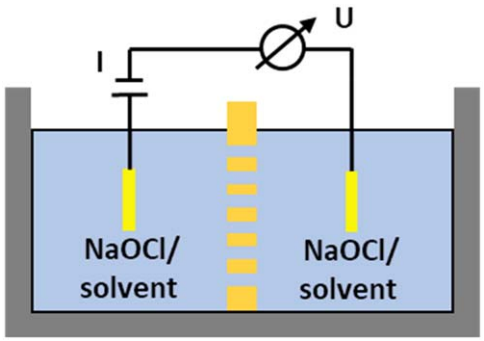

Figure 4. Experimental set-up for the fabrication of nanopores in PI membranes using of NaOCl/organic solvent mixture.

Table 1. Pore diameter D of PI samples pretreated with organic solvents, followed by track-etching with NaOCl solution. In case of elliptical shaped pores, the pore diameter was calculated by measuring the diameter of the minor axis.

Solvent	D (μm)
No ST	0.43 ± 0.02
MeOH	0.50 ± 0.04
ACN	0.88 ± 0.04
EtOH	0.89 ± 0.03
THF	1.46 ± 0.06
DMF	1.65 ± 0.07
DMSO	1.92 ± 0.09

nanopores in PI membranes by 47% (ACN), 31% (THF) and 6% (EtOH).

Another parameter to be considered when it comes to the fabrication of nanopores with different pore shapes, for example conical or bullet shaped nanopores, is the current increase speed after the breakthrough. In figure 5(f), the etching curves show faster current increase after breakthrough for all samples prepared with a mixture of NaOCl and organic solvent compared with the NaOCl etching solution. Note that the current increase in the case of THF is slightly faster than for ACN, although $\varepsilon_t^{\mathrm{NaOCl/ACN}} > \varepsilon_t^{\mathrm{NaOCl/THF}}$. One reason could be that the distribution of different etch rates ε_t is smaller in case of THF and a higher number of pores has the breakthrough at the same time. Another possible explanation is $\varepsilon_{xy}{}^{\mathrm{NaOCl/ACN}} < \varepsilon_{xy}{}^{\mathrm{NaOCl/THF}}$, which causes a faster pore diameter growth to allow higher ion flow. This indicates that, depending on the application of the PI membrane, it is important to choose a suitable organic solvent for nanopore fabrication.

The pore diameter is also determined after 45 min symmetrical etching at 50 °C using other etchant mixtures (9:1), i.e. NaOCl/MeOH, NaOCl/*i*-PrOH, NaOCl/DMF, NaOCl/DMSO, NaOCl/EtAc and NaOCl/DCM (figures 5(g), S8). Samples etched with NaOCl/DCM mixture showed a ~87% increase in pore diameter. The etching curve of DCM at 50 °C (figure S12(c)) shows a breakthrough during the first few minutes of the symmetrical etching indicating that $\varepsilon_t^{\mathrm{NaOCl/DCM}} \gg \varepsilon_{xy}{}^{\mathrm{NaOCl}}$. However, due to a limited controllability of the etching process, as well as the toxicity and high vapor pressure of DCM, only a few experiments are performed with this solvent (figures S11–S13, table S2). Figure S3(b) shows changes of the contact angle with etchant mixtures comprised of NaOCl and organic solvent (9:1) compared with data obtained for water or pure NaOCl solution. Again, it does not show any relationship between the wettability of the membrane surface with the etching solution and the pore diameter achieved in symmetrical etching.

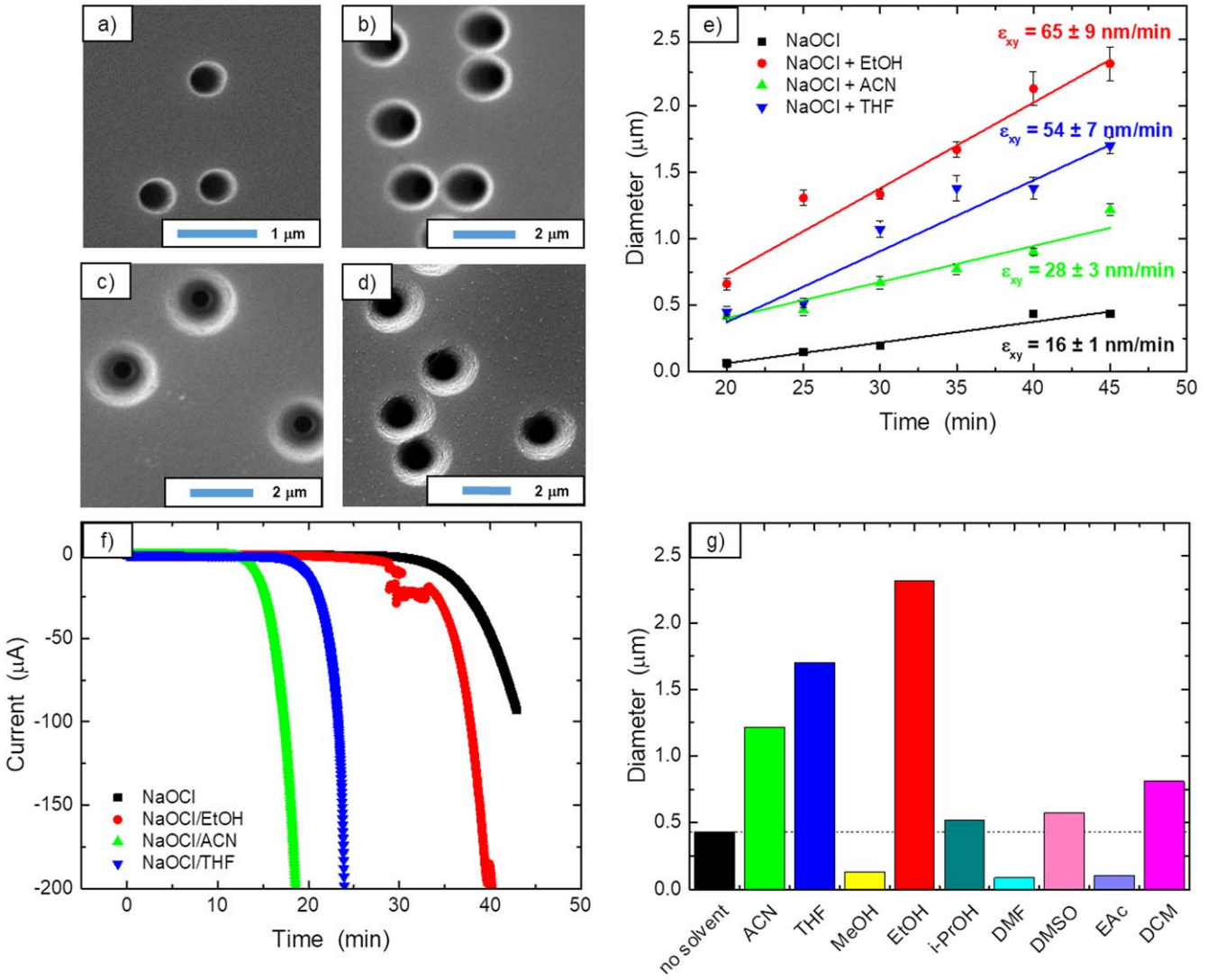

Figure 5. Symmetrical etching of PI membranes (10^7 pores cm^{-2}) with 12% NaOCl solution and 9:1 mixtures of NaOCl/solvents at 50 °C. SEM images after 45 min etching with (a) NaOCl, (b) NaOCl/ACN, (c) NaOCl/THF, and (d) NaOCl/EtOH. (e) Etch rates ε_{xy} of NaOCl and 9:1 mixtures of NaOCl/solvents at 50 °C calculated from at least five pore diameters in dependence of the etching time in symmetrical etching process. (f) Etching curves monitored during symmetrical etching process at 50 °C with NaOCl and 9:1 mixtures of NaOCl/solvents showing the breakthrough current related to the etch rates ε_t. (g) Effect of 10 vol% organic solvents in etchant mixtures with NaOCl on the pore diameter after 45 min symmetrical etching at 50 °C.

To conclude, etching at 50 °C with a NaOCl/solvent etchant mixture (9:1) is more efficient than with pure NaOCl solution in terms of generating larger pore diameters in a shorter time scale. The influence of the organic solvent on the etch rates ε_{xy} and ε_t not only depends on the solvent volume in the etching solution, but also on the organic solvent itself. Our results show that the order of etch rates of the bulk material is $\varepsilon_{xy}^{\mathrm{NaOCl/EtOH}} > \varepsilon_{xy}^{\mathrm{NaOCl/THF}} > \varepsilon_{xy}^{\mathrm{NaOCl/ACN}} > \varepsilon_{xy}^{\mathrm{NaOCl}}$, whereas the etch rate along the latent tracks is $\varepsilon_t^{\mathrm{NaOCl/ACN}} > \varepsilon_t^{\mathrm{NaOCl/THF}} > \varepsilon_t^{\mathrm{NaOCl/EtOH}} > \varepsilon_t^{\mathrm{NaOCl}}$. In terms of a fast pore fabrication, the controllability of the pore diameter growth, and also of health and environmental reasons, a mixture of NaOCl solution and ACN is the best choice among the solvents we tested.

3.2.2. Influence of organic solvent volume on pore diameter. Furthermore, the experiments are conducted by changing the volume (by vol%) of the organic solvents in the NaOCl solution. The SEM images and an overview of the pore diameter in dependence of the vol% of ACN, THF and EtOH are given in figure 6. Pore diameters of 2.00 ± 0.04 μm and 2.67 ± 0.16 μm are achieved by using NaOCl/ACN (8:2) and NaOCl/THF (7:3), respectively (table S1). Further increasing of the organic solvent volume (figure S10) reduced the pore diameters, probably due to a significant reduction of active chlorine concentration that is needed for the basic imide ring cleavage. In case of EtOH, the membrane surface shows extreme damages and dissolution when the solvent volume is increased up to 20%.

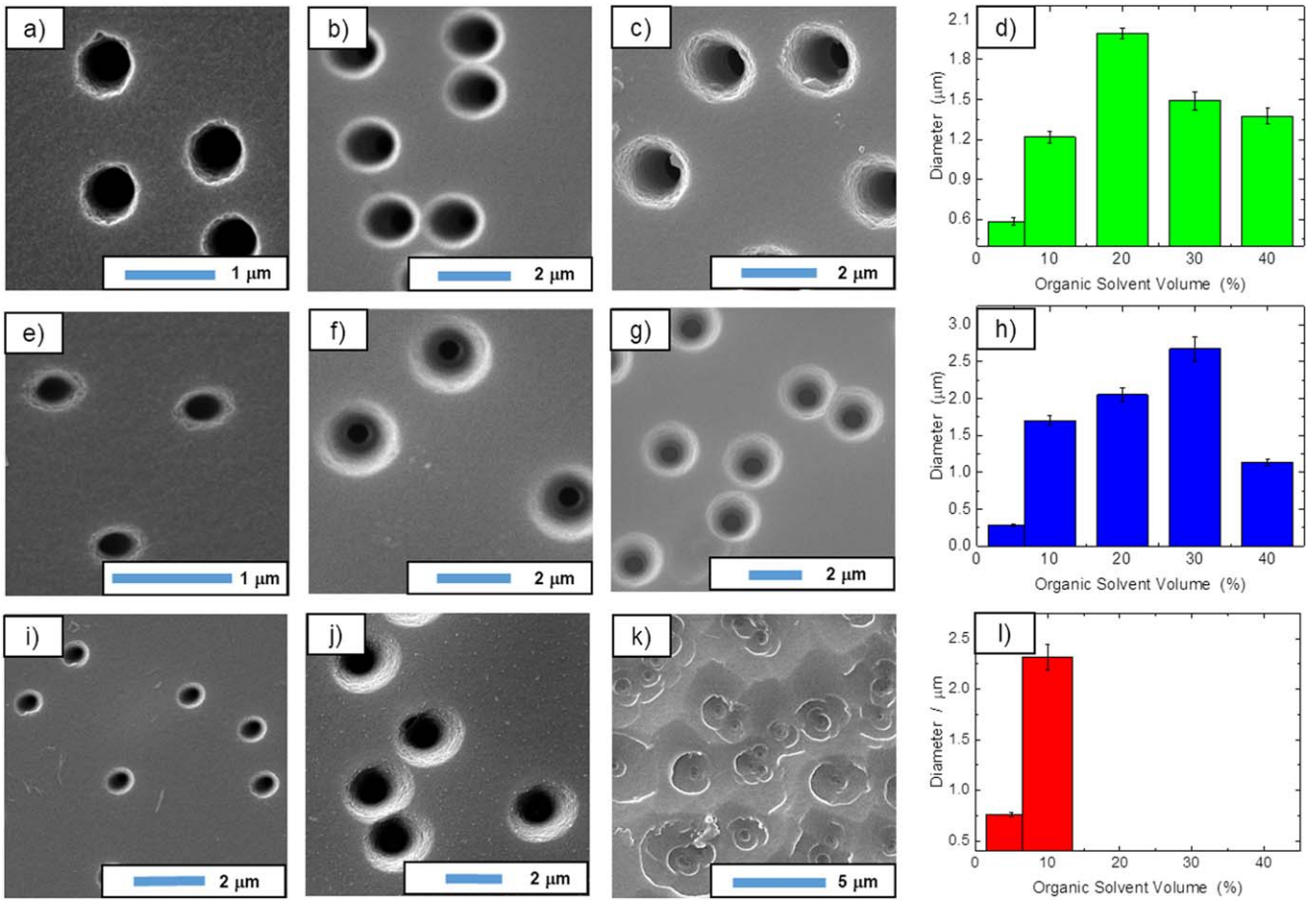

Figure 6. Solvent dependent symmetrical etching of PI membranes (10^7 pores cm^{-2}) with mixtures of NaOCl/solvent at 50 °C. SEM images after 45 min etching with 5%, 10% and 20% of ACN (a)–(c), THF (e)–(g) and EtOH (i)–(k), and the effect of NaOCl/organic solvent on the pore diameter in case of ACN (d), THF (h) and EtOH (I).

3.2.3. Influence of temperature on pore diameter. We also performed etching experiments at different temperatures to investigate the behavior of the etchant mixtures with organic solvents. Figure 7 shows SEM images and an overview of the pore diameters in dependence of the etching temperature of PI membranes, which were symmetrically etched for 45 min at 23 °C (room temperature), 35 °C and 50 °C with an etchant mixture of NaOCl/solvent (9:1) containing ACN, THF and EtOH.

At room temperature (23 °C), the nanopores (36 ± 2 nm) are visible under SEM only in the case of NaOCl/ACN etched sample. While, the samples etched with NaOCl/THF and NaOCl/EtOH mixtures did not show any pores. It is possible that smaller pores are closed during the Au sputtering process used for SEM sample preparation. At 35 °C, an increase in pore diameters indicate that the bulk-etch rate (ε_{xy}) of the material is $\varepsilon_{xy}^{\mathrm{NaOCl/EtOH}} > \varepsilon_{xy}^{\mathrm{NaOCl/THF}} > \varepsilon_{xy}^{\mathrm{NaOCl/ACN}} > \varepsilon_{xy}^{\mathrm{NaOCl}}$. Regarding the etching curves (figures S12, S13), the etch rates along the latent tracks are quite similar ($\varepsilon_{\mathrm{t}}^{\mathrm{NaOCl/THF}} \approx 188$ nm min^{-1} and $\varepsilon_{\mathrm{t}}^{\mathrm{NaOCl/ACN}} \approx 222$ nm min^{-1}), whereas no breakthrough point was reached in 45 min of symmetrical etching with NaOCl/EtOH mixture and NaOCl solutions.

3.3. Determination of the pore geometry

Since organic solvents have a significant influence on the etch rates, i.e. ε_{xy} and ε_{t} of heavy ion irradiated PI membranes, the impact of organic solvent on the nanopore geometry is also analyzed. For this purpose, the PI membranes (10^7 pores cm^{-2}) are etched under symmetric and asymmetric track-etching conditions at 50 °C for 45 min using 9:1 etchant mixtures of NaOCl/ACN, NaOCl/THF and NaOCl/EtOH (figure S14). In case of asymmetrical track-etching, a stopping solution mixture comprised of 1 M KI/solvent (9:1) was used to neutralize the etchant after the breakthrough point. Figure 8 shows cross sections of PI membranes prepared using NaOCl/ACN and NaOCl/THF as etchant mixtures.

After 45 min of symmetrical etching at 50 °C with etchant mixtures of 9:1 NaOCl/ACN (figure 8(a)) and NaOCl/THF (figure 8(c)), the almost cylindrical shaped pores were successfully fabricated in both PI samples. Note that it is quite challenging to prepare the PI membrane samples to image cross-section of the nanopore. Therefore, nanopore cross-section geometry was slightly deformed due to the sample preparation for SEM analysis.

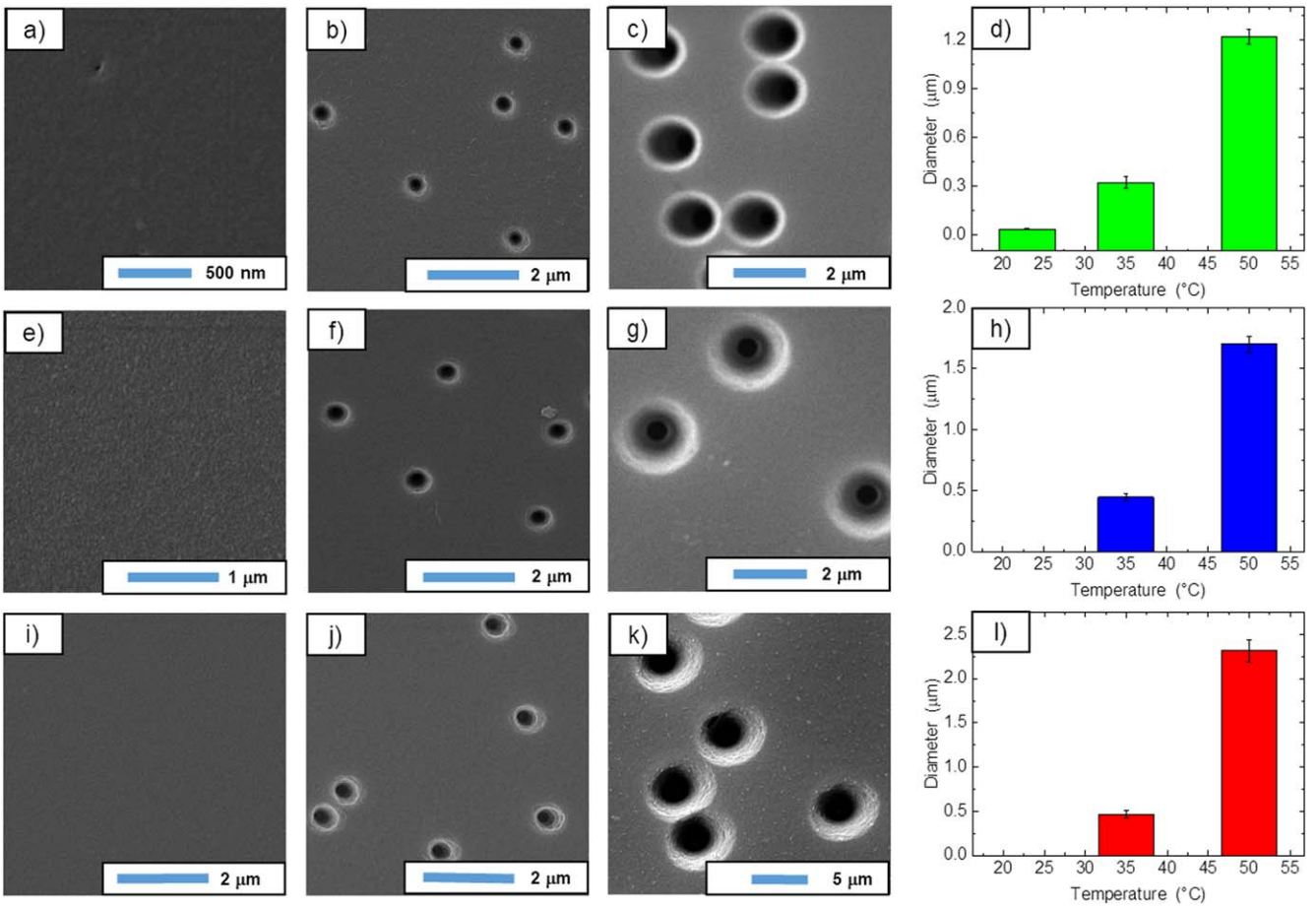

Figure 7. Temperature dependent symmetrical etching of PI membranes (10^7 pores cm^{-2}) with an etchant mixture of NaOCl/solvent (9:1). SEM images after 45 min etching at 23 °C, 35 °C and 50 °C with ACN (a)–(c), THF (e)–(g) and EtOH (i)–(k), and the effect of the etching temperature on the pore diameter in the case of ACN (d), THF (h) and EtOH (l).

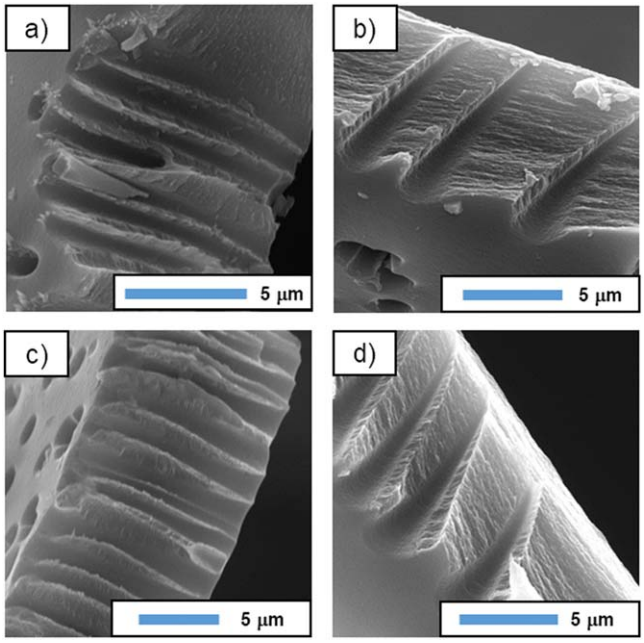

Figure 8. SEM images of PI membranes (10^7 pores cm^{-2}) prepared using symmetrical and asymmetrical track-etching technique with 9:1 etchant mixtures of NaOCl/ACN (a), (b) and NaOCl/THF (c), (d) at 50 °C for 45 min chemical etching.

In case of asymmetrical track-etching for ~45 min with NaOCl/ACN (figure 8(b)) and NaOCl/THF mixture (figure 8(d)), the asymmetric shaped nanopores were successfully formed across the membrane length. For the case of NaOCl/THF, the base opening diameter of the asymmetric nanopore is larger compared to NaOCl/ACN etchant mixture. On the contrary, the PI samples prepared with NaOCl/EtOH did not reach a breakthrough point in 45 min of asymmetric-etching time (figure S15). Still, the profile of the etched area indicates a conical pore geometry. Despite possible deformations during sample preparation, the SEM images in figure 8 clearly show the effect of organic solvents on the ion track-etching of PI membranes compared to those prepared using pure NaOCl solution (figure S15).

Comparing the inner pore wall structure of the nanopores in figures 8 and S16, the nanopore surface of the samples prepared by using etchant mixtures is smooth and more homogenous than samples etched via the solvent pretreatment.

3.4. Fabrication of single-nanopore membranes

The polymer membranes having a single conical nanopore have been employed to miniaturize very sensitive and selective nanofluidic devices for successful recognition of (bio) molecules [29, 43, 53]. With this background, the organic

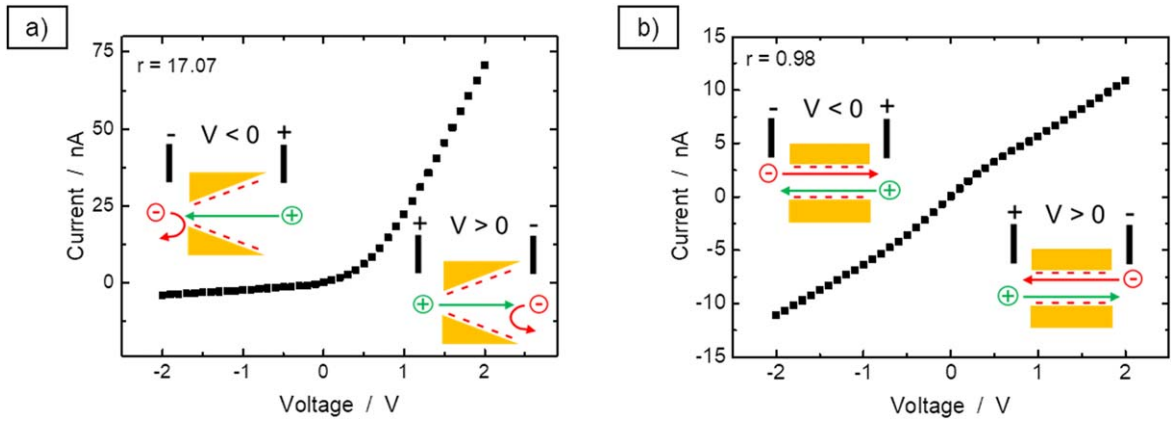

Figure 9. *I–V* characteristics of a PI (a) single asymmetric nanopore and (b) single cylindrical nanopore membrane prepared by using 9:1 etchant mixtures of NaOCl/ACN. The electrolyte solution used for the *I–V* measurements is 0.1 M KCl. The inset in the Figures shows the mechanism of ion transport process across the single-nanopore membranes under applied potential.

solvent-assisted track-etching of PI membranes is further extended to enhance the fabrication of single cylindrical- and conical-shaped nanopores under symmetric and asymmetric conditions at 50 °C, respectively. The *I–V* measurements of the single-pore membrane are performed in 0.1 M KCl electrolyte (figure 9).

The ion track-etched PI membranes contain carboxylic acid groups on the nanopore walls, which import negative fixed charges on the pore surface under physiological conditions [43]. The single conical nanopore exhibit ion current rectification due to asymmetric geometry and negative charges under applied potential. It means that cations preferentially flow from tip to base side of the conical nanopore as shown in figure 9(a). The cylindrical nanopore exhibits ohmic characteristics (linear *I–V* curve) because of the absence of asymmetry although the pore surface is negatively charged as shown in figure 9(b) [29]. Moreover, the ion flow through cylindrical nanopore experience more resistance compared to conical ones. That's why the conical pore shows higher value of ion current at positive potential than the cylindrical nanopore (figure 9). In the case of conical nanopores, the rectification behavior is quantified by the current rectification ratio $r = |I(+2\text{ V})|/I(-2\text{ V})$ [43, 54, 55].

I–V measurements of PI membranes with asymmetric single nanopores prepared after pretreatment with DMF and THF or by using 9:1 etchant mixtures of NaOCl/ACN and NaOCl/THF show *I–V* curves with diode-like behavior (figures 9(a), S17). In case of the pretreatment step, the *I–V* curves exhibit high ion currents at +2 V (>130 nA) and small currents at −2 V (<−10 nA) with $r > 19.5$. In contrast, the single-nanopore membranes prepared by using etchant mixtures resulted in much smaller ion currents at +2 V (<75 nA) and −2 V (<−5 nA) and smaller rectification ratios ($r^{\text{NaOCl/ACN}} = 17.07$ and $r^{\text{NaOCl/THF}} = 11.7$). In addition to asymmetric geometry and fixed charges on the pore surface, the cone angle is another parameter which should also be considered to determine the extent of ion current rectification characteristics of the single conical nanopore. Unfortunately, we are not yet sure about the cone angle of the conical nanopores prepared using organic solvent assisted asymmetric etching. Therefore, the relationship between ion current rectification and cone angle could not be established based on this study. The SEM imaging of tip opening of the conical nanopores in the polymeric membrane is exceedingly difficult because the charging of the sample at low resolution can deflect the scanning beam.

The experimental results show that both approaches described in sections 3.1. and 3.2. can be used to fabricate asymmetrically shaped single nanopores in PI membranes with diode-like properties. This clearly shows that the effect of organic solvents on the chemical etching of ion tracks is independent of the latent track density.

4. Conclusion

In summary, the role of organic solvents in the track-etching of heavy ion irradiated PI membranes is demonstrated. The organic solvents have been either used for sample pretreatment before the chemical etching process (two-step etching) or directly added in the chemical etchant (NaOCl) solution (one-step etching) and led to the fabrication of PI membranes with larger pore diameters compared to chemical etching with NaOCl under the same experimental conditions. For two-step etching process, the order of increase in pore diameter was found to be DMSO (1.92 μm) > DMF (1.65 μm) > THF (1.46 μm) > ACN (0.88 μm) ≈ EtOH (0.89 μm) > MeOH (0.50 μm) ≈ no solvent (0.43 μm). In the case of etchant mixture (NaOCl/solvent; 9:1), a significant increase in both the bulk- (ε_{xy}) and track-etch (ε_t) rates was noticed. In the one-step etching approach, the bulk-etch rate was found to be in the order of $\varepsilon_{xy}^{\text{NaOCl/EtOH}}$ (65 ± 9 nm min^{-1}) > $\varepsilon_{xy}^{\text{NaOCl/THF}}$ (54 ± 7 nm min^{-1}) > $\varepsilon_{xy}^{\text{NaOCl/ACN}}$ (28 ± 3 nm min^{-1}) > $\varepsilon_{xy}^{\text{NaOCl}}$ (16 ± 1 nm min^{-1}), whereas the order of track-etch rate was $\varepsilon_t^{\text{NaOCl/ACN}}$ (353 nm min^{-1}) > $\varepsilon_t^{\text{NaOCl/THF}}$ (273 nm min^{-1}) > $\varepsilon_t^{\text{NaOCl/EtOH}}$ (200 nm min^{-1}) > $\varepsilon_t^{\text{NaOCl}}$ (188 nm min^{-1}). Among the various etchant compositions, a dramatic enhancement in the track-etch rates was obtained by using THF and ACN solvents, resulting in the reduction of the nanopore fabrication time up to 31% and

47%, respectively. In the past, PET nanopores were favored in sensing applications despite the superior chemical and mechanical stability of PI, because of fast PET track-etching process. This study opens up new opportunities for using PI nanopores in different possible applications, not only because the use of organic solvents significantly reduced the fabrication time, but also because of the flexibility of this method to fabricate nanopores of various dimensions.

Acknowledgments

The authors acknowledge the support from the LOEWE project iNAPO, Hessen State Ministry of Higher Education, Research and the Arts, Germany. Special thanks to Alena Bell (Dept. of Material- and Geo-Sciences, Physics of Surfaces) for her help with instrumentation of contact angle measurements, and Prof C Trautmann and Dr E Toimil Molares (GSI, Material Research Department) for their support with the heavy ion irradiation experiments. The heavy ion irradiation is based on a UMAT experiment, which was performed at the X0-beamline of the UNILAC at the GSI Helmholtzzentrum fuer Schwerionenforschung, Darmstadt (Germany) in the frame of FAIR Phase-0.

Data availability statement

All data that support the findings of this study are included within the article (and any supplementary files).

ORCID iDs

Kristina Froehlich https://orcid.org/0000-0003-4352-5176

References

[1] Stoloff D H and Wanunu M 2013 *Curr. Opin. Biotechnol.* **24** 699–704
[2] Pérez-Mitta G, Peinetti A S, Cortez M L, Toimil-Molares M E, Trautmann C and Azzaroni O 2018 *Nano Lett.* **18** 3303–10
[3] Keyser U F 2016 *Nat. Nanotechnol.* **11** 106–8
[4] Varongchayakul N, Hersey J, Squires A, Meller A and Grinstaff M 2018 *Adv. Funct. Mater.* **28** 1804182
[5] Ali M, Nasir S, Froehlich K, Ramirez P, Cervera J, Mafe S and Ensinger W 2021 *Adv. Mater. Interfaces* **8** 2001766
[6] Froehlich K, Nasir S, Ali M, Ramirez P, Cervera J, Mafe S and Ensinger W 2021 *J. Membr. Sci.* **617** 118633
[7] McAllister A B, Menchaca C X, Freeman J, Chen R and Shen M 2018 *J. Electrochem. Soc.* **165** G3093–8
[8] Prabhu A S, Jubery T Z N, Freedman K J, Mulero R, Dutta P and Kim M J 2010 *J. Phys. Condens. Matter* **22** 454107
[9] Zhang Y, He Y, Tsutsui M, Miao X S and Taniguchi M 2017 *Sci. Rep.* **7** 46661
[10] Zhang H, Tian Y and Jiang L 2016 *Nano Today* **11** 61–81
[11] Li J, Stein D, McMullan C, Branton D, Aziz M J and Golovchenko J A 2001 *Nature* **412** 166–9
[12] Liu S *et al* 2013 *Adv. Mater.* **25** 4549–54
[13] Storm A J, Chen J H, Ling X S, Zandbergen H W and Dekker C 2003 *Nat. Mater.* **2** 537–40
[14] Venkatesan B M, Shah A B, Zuo J M and Bashir R 2010 *Adv. Funct. Mater.* **20** 1266–75
[15] Apel P Y 2001 *Radiat. Meas.* **34** 559–66
[16] Garaj S, Hubbard W, Reina A, Kong J, Branton D and Golovchenko J A 2010 *Nature* **467** 190–3
[17] Wang G, Bohaty A K, Zharov I and White H S 2006 *J. Am. Chem. Soc.* **128** 13553–8
[18] White R J, Ervin E N, Yang T, Chen X, Daniel S, Cremer P S and White H S 2007 *J. Am. Chem. Soc.* **129** 11766–75
[19] Fornasiero F, In J B, Kim S, Park H G, Wang Y, Grigoropoulos C P, Noy A and Bakajin O 2010 *Langmuir* **26** 14848–53
[20] Chen R, Hu K, Yu Y, Mirkin M V and Amemiya S 2016 *J. Electrochem. Soc.* **163** H3032–7
[21] Liebes-Peer Y, Bandalo V, Sökmen Ü, Tornow M and Ashkenasy N 2016 *Microchim. Acta* **183** 987–94
[22] Kwok H, Briggs K and Tabard-Cossa V 2014 *PLoS One* **9** e92880
[23] Bell N A W, Thacker V V, Hernández-Ainsa S, Fuentes-Perez M E, Moreno-Herrero F, Liedl T and Keyser U F 2013 *Lab Chip* **13** 1859–62
[24] Deng T, Li M, Wang Y and Liu Z 2015 *Sci. Bull.* **60** 304–19
[25] Siwy Z, Apel P, Dobrev D, Neumann R, Spohr R, Trautmann C and Voss K 2003 *Nucl. Instrum. Methods Phys. Res.* B **208** 143–8
[26] Juan W H 1994 *J. Vac. Sci. Technol.* B **12** 422–6
[27] Kong Y, Lin Y and Dong Z 2021 *China Semiconductor Technology Int. Conf. (CSTIC)*
[28] Chen Q and Liu Z 2019 *Sensors* **19** 1886
[29] Lepoitevin M, Ma T, Bechelany M, Janot J-M and Balme S 2017 *Adv. Colloid Interface Sci.* **250** 195–213
[30] Apel P Y 1995 *Radiat. Meas.* **25** 667–74
[31] Apel P Y, Blonskaya I V, Cornelius T W, Neumann R, Spohr R, Schwartz K, Skuratov V A and Trautmann C 2009 *Radiat. Meas.* **44** 759–62
[32] Apel P Y, Blonskaya I V, Didyk A Y, Dmitriev S N, Orelovitch O L, Root D, Samoilova L I and Vutsadakis V A 2001 *Nucl. Instrum. Methods Phys. Res.* B **179** 55–62
[33] Apel P Y, Blonskaya I V, Dmitriev S N, Orelovitch O L, Presz A and Sartowska B A 2007 *Nanotechnology* **18** 305302
[34] Vilensky A I, Zagorski D L, Kabanov V Y and Mchedlishvili B V 2003 *Radiat. Meas.* **36** 131–5
[35] Harrell C C, Siwy Z S and Martin C R 2006 *Small* **2** 194–8
[36] Scopece P, Baker L A, Ugo P and Martin C R 2006 *Nanotechnology* **17** 3951–6
[37] Verker R, Grossman E and Eliaz N 2009 *Acta Mater.* **57** 1112–9
[38] Li R, Li C, He S, Di M and Yang D 2008 *Radiat. Phys. Chem.* **77** 482–9
[39] Gupta S K, Gupta R, Singh P, Kumar V, Jaiswal M K, Chakarvarti S K and Kumar R 2017 *Nucl. Instrum. Methods Phys. Res.* B **406** 188–92
[40] Barshilia H C, Ananth A, Gupta N and Anandan C 2013 *Appl. Surf. Sci.* **268** 464–71
[41] Chahadih A, Cresson P Y, Hamouda Z, Gu S, Mismer C and Lasri T 2015 *Sensors Actuators* A **229** 128–35
[42] Siwy Z, Apel P, Baur D, Dobrev D D, Korchev Y E, Neumann R, Spohr R, Trautmann C and Voss K-O 2003 *Surf. Sci.* **532–535** 1061–6
[43] Ali M, Schiedt B, Healy K, Neumann R and Ensinger W 2008 *Nanotechnology* **19** 85713
[44] Trautmann C, Briichle W, Spohr R, Vetter J and Angert N 1996 *Nucl. Instrum. Methods Phys. Res.* B **11** 70–4

[45] Klintberg L, Lindeberg M and Thornell G 2001 *Nucl. Instrum. Methods Phys. Res.* B **184** 536–43
[46] Ohya H, Kudryavtsev V and Semenova S 1996 *Polyimide Membranes: Applications, Fabrications and Properties* (Tokyo: Kodansha/Gordon and Breach)
[47] Cornelius T W, Apel P Y, Schiedt B, Trautmann C, Toimil-Molares M E, Karim S and Neumann R 2007 *Nucl. Instrum. Methods Phys. Res.* B **265** 553–7
[48] Kaya D and Keçeci K 2020 *J. Electrochem. Soc.* **167** 37543
[49] Apel P Y, Blonskaya I V, Orelovitch O L, Sartowska B A and Spohr R 2012 *Nanotechnology* **23** 225503
[50] Guo L, Wang L and Wang Y 2016 *Chem. Commun.* **52** 6899–902
[51] Ogieglo W, Wormeester H, Eichhorn K-J, Wessling M and Benes N E 2015 *Prog. Polym. Sci.* **42** 42–78
[52] Lee C K, Diesendruck C E, Lu E, Pickett A N, May P A, Moore J S and Braun P V 2014 *Macromolecules* **47** 2690–4
[53] Zhang S, Chen W, Song L, Wang X, Sun W, Song P, Ashraf G, Liu B and Zhao Y-D 2021 *Sensors Actuators* A **3** 100042
[54] Apel P Y, Korchev Y E, Siwy Z, Spohr R and Yoshida M 2001 *Nucl. Instrum. Methods Phys. Res.* B **184** 337–46
[55] Lin C-Y, Ma T, Siwy Z S, Balme S and Hsu J-P 2020 *J. Phys. Chem. Lett.* **11** 60–6